ARTICLE

Anisotropic Hydrogen Etching of Chemical Vapor Deposited Graphene

Yi Zhang,[†,‡,⊥] Zhen Li,[†,⊥] Pyojae Kim,[†] Luyao Zhang,[§] and Chongwu Zhou[†,‡,§,*]

[†]Department of Electrical Engineering, [‡]Department of Chemistry, and [§]Department of Material Science, University of Southern California, Los Angeles, California 90089, United States [⊥]These authors contributed equally to this work.

ABSTRACT

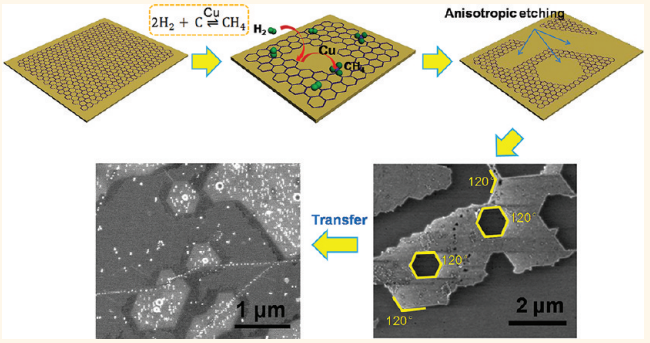

We report a simple, clean, and highly anisotropic hydrogen etching method for chemical vapor deposited (CVD) graphene catalyzed by the copper substrate. By exposing CVD graphene on copper foil to hydrogen flow around 800 °C, we observed that the initially continuous graphene can be etched to have many hexagonal openings. In addition, we found that the etching is temperature dependent. Compared to other temperatures (700, 900, and 1000 °C), etching of graphene at 800 °C is most efficient and anisotropic. Of the angles of graphene edges after etching, 80% are 120°, indicating the etching is highly anisotropic. No increase of the D band along the etched edges indicates that the crystallographic orientation of etching is in the zigzag direction. Furthermore, we observed that copper played an important role in catalyzing the etching reaction, as no etching was observed for graphene transferred to Si/SiO_2 under similar conditions. This highly anisotropic hydrogen etching technology may work as a simple and convenient way to determine graphene crystal orientation and grain size and may enable the etching of graphene into nanoribbons for electronic applications.

KEYWORDS: CVD graphene · hydrogen etching · anisotropic · copper-catalyzed

Graphene, a two-dimensional, honeycomb arrangement of carbon atoms, has drawn significant attention with its interesting physical properties.[1−3] In terms of the preparation of graphene, chemical vapor deposition (CVD) has raised its popularity as a scalable and cost-effective approach for graphene synthesis.[4−11] Among various CVD approaches, since the debut of CVD graphene synthesis using copper as a substrate reported by Li *et al.*,[9] the copper-catalyzed decomposition of methane to form graphene has been studied from a variety of aspects.[12−15] It is well known that single-layer graphene (SLG) is formed on a copper foil substrate by decomposition of methane, resulting in the formation of graphene and hydrogen. The roles of various parameters such as pressure[12] and hydrogen[16] in chemical vapor deposition of graphene have been studied in some recent papers. One can imagine that the reverse reaction could also occur by exposing graphene to hydrogen and would effectively result in etching. However, the reverse reaction has not been systematically studied, such as the role of temperature and copper substrate, even though etching using other processes such as gas phase chemical etching[17] and hydrogen plasma etching[18,19] has led to important applications including formation of graphene nanoribbons.

In this work, we have studied anisotropic hydrogen etching of chemical vapor deposited graphene as the reverse reaction of graphene growth. We observed that continuous graphene could be etched into hexagonal openings by exposing CVD graphene on copper foil to hydrogen flow at high temperatures. The etching is found to be temperature-dependent, and 800 °C offers the most efficient and anisotropic etching. Of the angles of graphene edges after etching at 800 °C, 80% are 120°. We assigned the etched edges to ⟨1120⟩ edges, which are the zigzag edges of graphene. Moreover, we observed that copper played an important role in catalyzing the etching reaction, as no etching was observed for graphene transferred to Si/SiO_2 substrate under similar conditions. This highly anisotropic hydrogen etching technology may work as a simple and convenient way to determine graphene grain size and crystal orientation and may enable the etching of graphene into nanoribbons with smooth and ordered zigzag edges without compromising the quality of graphene.

* Address corresponding to chongwuz@usc.edu.

Received for review August 6, 2011 and accepted October 19, 2011.

Published online 10.1021/nn202996r

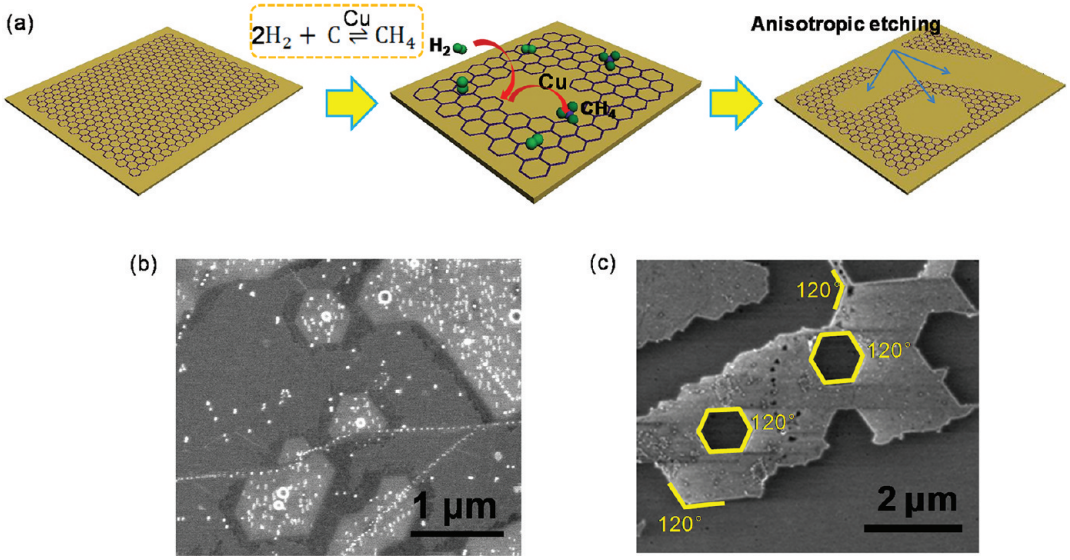

Figure 1. (a) Schematic diagram of Cu etching mechanism. (b) SEM image of graphene after etching on copper foil and (c) transferred onto a Si/SiO_2 substrate.

RESULTS AND DISCUSSION

Our work started with the preparation of CVD graphene. SLG was grown on copper foil using CVD similar to the process reported by Li *et al.*[9] (see details in Methods section). After the synthesis of CVD graphene, anisotropic etching of graphene was done in the same CVD chamber at 800 °C with the flow of hydrogen. As F1 illustrated in Figure 1, the etching reaction is the reverse reaction of graphene growth, as hydrogen can react with carbon in graphene and produce methane. We observed that almost every etched hexagon had a particle in the center, as shown in the left SEM image in Figure 1. The particles are believed to come from the quartz tube used in the CVD chamber, and the etching reaction is initiated by breaking the carbon−carbon bond of graphene in locations they were deposited. Energy-dispersive X-ray spectroscopy has been performed to test the composition of the particles (Figure S1). Strong silicon and oxygen peaks from the spectrum taken on one of the particles indicate that the particles are silicon dioxide.

After small openings were etched on graphene, the copper substrate underneath would serve as a catalyst for hydrogen to react with carbon in graphene and, hence, accelerate the etching reaction of graphene. Interestingly, the catalytic etching reaction is highly anisotropic in our experimental conditions. As shown in the SEM image in Figure 1c taken of the graphene transferred to a Si/SiO_2 substrate, the openings in graphene after etching turn out to be very regular hexagonal shaped, and edges with 120° angles can be found in many etched corners. While we report hydrogen etching of graphene on a copper substrate in this paper, a similar reaction may occur for graphene on other substrates such as nickel. Even though the SiO_2 nanoparticles in our current work are randomly located, controlled positioning of SiO_2 nanoparticles can be achieved by combining patterning and deposition of SiO_2 particles. For instance, by using assembled nanospheres as a shadow mask for SiO_2 deposition, one should achieve SiO_2 particle deposition at desired locations.[20] Alternatively, our observed hydrogen etching of graphene may also work after initiating openings in graphene via patterning and oxygen plasma etching.[19]

We have conducted micro-Raman microscopy on both as-grown CVD graphene and graphene after the etching reaction. As-grown graphene was transferred onto a 300 nm Si/SiO_2 substrate using the reported transfer technique.[8] As shown in the SEM image after transfer in Figure 2a, the graphene is continuous, clean, F2 and uniform over a large area. Raman spectra were collected over the entire substrate to determine the number of layers, as well as the quality of graphene. The inset of Figure 2a shows a typical Raman spectrum of the as-transferred graphene. The I_{2D}/I_G intensity ratio is 2.2, and the 2D peak has a full width at half-maximum (fwhm) of ~33 cm^{-1}, which confirms the formation of SLG.[9] The absence of a D peak indicates that the graphene after transfer maintains high quality. Figure 2b shows the SEM image of graphene etched at 800 °C after transfer. Raman spectra were taken from the remaining graphene and one of the etched hexagons, respectively. The red curve in the inset of Figure 2b represents the Raman spectrum of the remaining graphene (pointed by the red arrow), which does not show the presence of a D peak, indicating the remaining graphene after etching has few defects.[21,22] The blue curve represents the Raman spectrum inside the etched hexagons (pointed by the blue arrow), which almost does not show any G and 2D band intensity, indicating the removal of graphene by anisotropic etching of hydrogen.

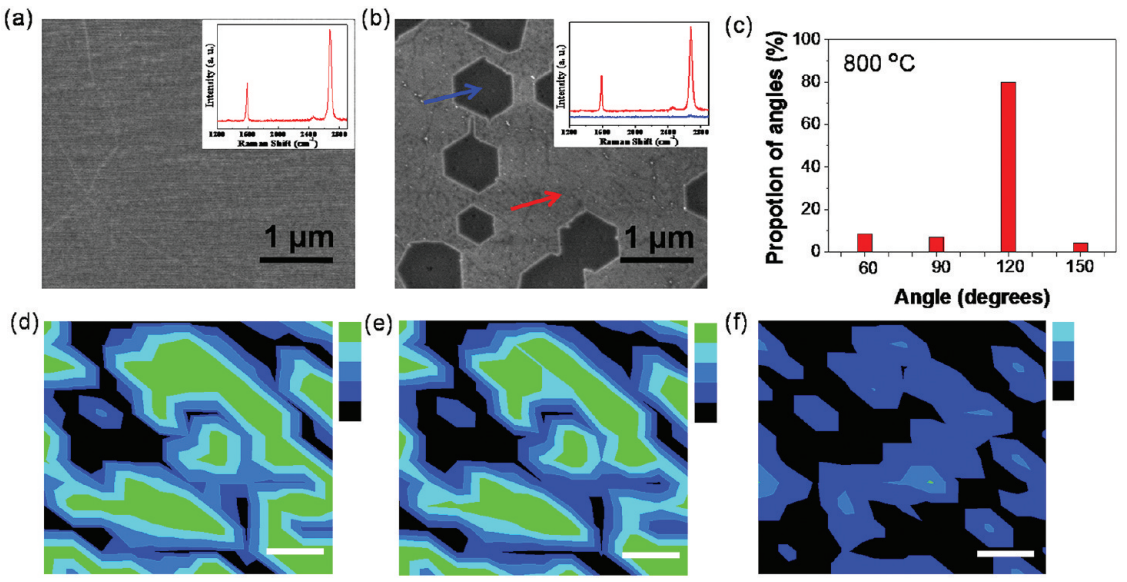

Figure 2. CVD graphene before and after etching. (a) As-grown CVD graphene transferred onto Si/SiO_2 and a representative Raman spectrum as an inset; (b) graphene etched by H_2 at 800 °C and transferred onto Si/SiO_2. Raman spectra (inset) show the intact graphene (pointed by red arrow) and etched region (pointed by blue arrow). (c) Histogram of proportion of angles of graphene etched edges. (d–f) Raman map of I_G (d) (color scale bar: 100, 200, 500, 800, >800 au), I_{2D} (e) (color scale bar: 300, 900, 1500, 2200, >2200 au), and I_D (f) (color scale bar: 40, 80, 120, >120 au). The scale bar for d–f is 3 μm.

We also studied the orientation of the etching by measuring the angles of graphene edges after etching. As shown in Figure 2c, 80% of the 139 measured angles were 120°, indicating that the etching is along the specific crystal orientation of graphene. It was reported that the pitting and channeling by metal[23−27] and SiO_2[28] nanoparticles tended to happen along the $\langle 11\bar{2}0 \rangle$ direction, which corresponded to the zigzag edge of graphene The theoretical study also reveals that in the graphene gasification reaction, since the C–C bond on the armchair face is the weakest one, it is more amenable to cleavage compared to the C–C bond on the zigzag face.[25,29] Therefore, we can assign the etching orientation to the zigzag face of graphene. From the result shown in Figure 2c, we can conclude that the copper-assisted hydrogen etching is highly anisotropic and efficient, which etches graphene along the zigzag direction.

We further investigated the surface of etched graphene by Raman surface mapping. The step of Raman surface mapping was 1.5 μm, in both the X and Y direction. Figure 2d–f are Raman maps of I_G, I_{2D}, and I_D, respectively. I_G and I_{2D} maps show the anisotropic behavior of the etched patterns, which mostly have edges of 120°. The I_D map in Figure 2f shows that D peak intensity is uniform over the remaining graphene area. Raman spectra taken from selected regions across etched edges are shown in Figure S2. Figure S2a shows a SEM image of etched graphene, with letters A to D indicating locations inside graphene (A and D) and at the etched edges (B and C). Figure S2b shows corresponding Raman spectra taken from location A to D. The D band in each spectrum is low no matter whether the spectrum is taken from the inside region of graphene (A and D) or from the edge of the remaining graphene (B and C). Figure S2c shows a plot of D band intensity of spectra taken from A to D. We can tell that the D band intensity at the edges of remaining graphene does not increase compared to the inner region, indicating that the edges are smooth and along the zigzag direction.[16,30]

Temperature always plays a significant role in chemical reactions. For a better understanding of the etching process, we studied the influence of temperature in the catalytically etching reaction. Four different temperatures were investigated in our experiment. The SLG samples used in the etching experiments were prepared in the same round of growth reaction, ensuring the uniformity and consistency of the starting SLG in each etching reaction.

After etching at 700 °C for 30 min, the etching was observed to be mild and is probably along the grain boundaries of graphene, therefore leading to graphene islands, shown in Figure 3a and b using different magnifications. Only a small amount of etched hexagons is observed inside the graphene islands after etching at 700 °C for 30 min. When 800 °C was used for etching, a larger area of graphene was etched away, and the etched patterns were mostly hexagonal, as seen in Figure 3c and d. We could also observe that the edges of etched graphene were mostly 120° in Figure 3d. When 900 °C was used for etching, we observed a decrease of the etched area of graphene, as well as fewer anisotropic etched patterns. When the temperature was further brought up to 1000 °C, the percentage of etched graphene became even lower.

The edge of the etched patterns became round, indicating a decrease of the anisotropic property of the etching. We did not observe any etching effect when the temperature decreased to 600 °C, and it can be understood, as the etching reaction will only happen when the temperature reaches a certain point to overcome the activation energy of the breaking of carbon–carbon bonds. On the other hand, since the etching reaction is exothermic, the reaction is unfavorable if the reaction temperature is very high. That is why we observed the weakening of the etching effect when the temperature increased to 900 and 1000 °C. The decrease of the anisotropic property of etching can also be attributed to the increase of temperature. On the basis of the theoretical calculation of hydrogen addition to zigzag and armchair edges,[29] the cleavage of the C–C bond from the armchair edge is much easier than from the zigzag edge. Therefore, when the temperature is relatively low, the selectivity between etching from a zigzag edge and etching from an armchair edge is high since the activation energy of breaking the C–C bond from the armchair edge is much lower. When the temperature is high enough to overcome the energy barrier of breaking the C–C bond from the zigzag edge, the anisotropic behavior of the etching process is much weakened. This explains why we observed that the anisotropic behavior became less pronounced when the temperature was enhanced from 800 °C to 900 °C and then 1000 °C.

We further calculated the percentage of the etched area of graphene at different temperatures. Five different regions from the samples were randomly picked for each temperature for the calculation of the etched area, and the size of each region was 40 μm × 30 μm. According to the histograms in Figure 4a–d, we could tell that the percentage of etched area of graphene increased from 700 °C to 800 °C, but then dropped

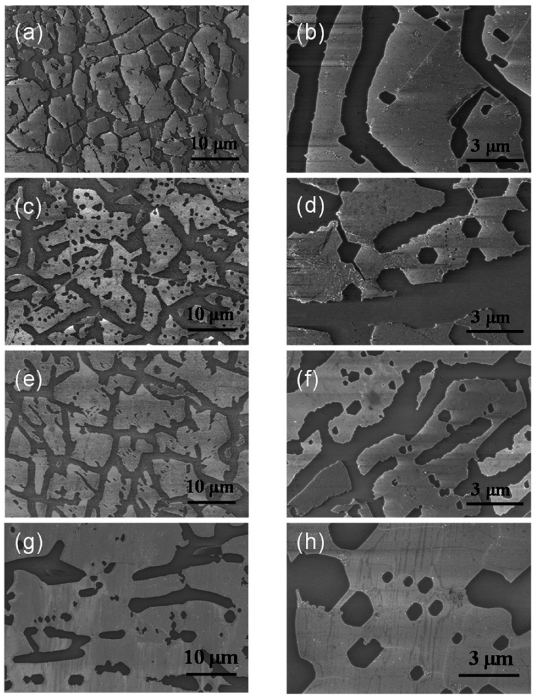

Figure 3. SEM images at different magnifications of graphene etched at different temperatures and transferred onto a Si/SiO_2 substrate: (a and b) 700 °C; (c and d) 800 °C; (e and f) 900 °C; (g and h) 1000 °C.

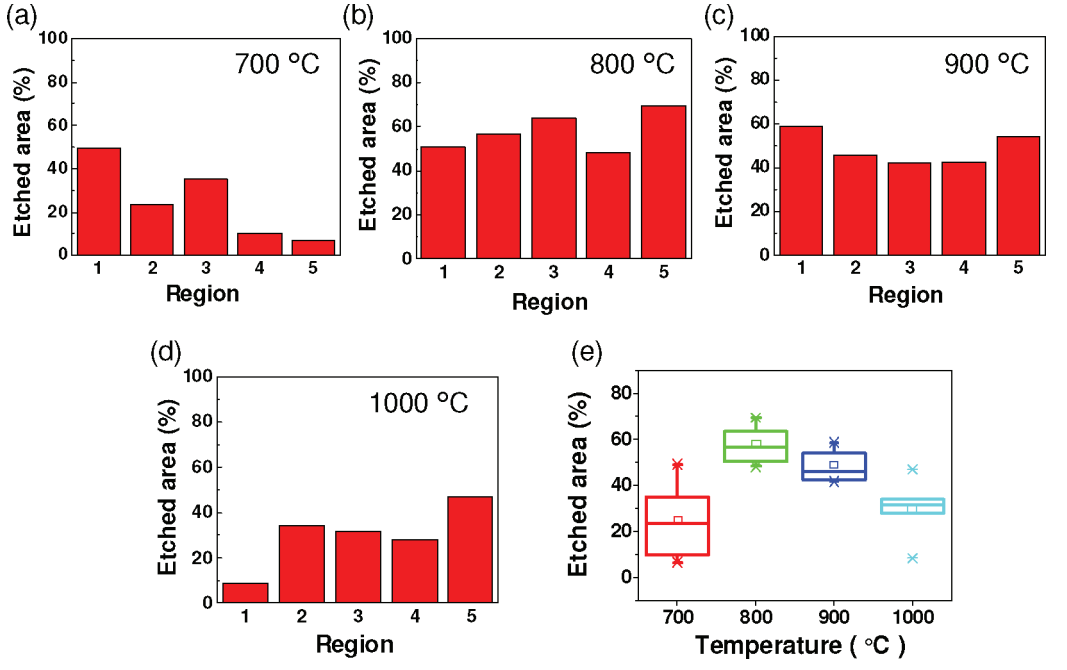

Figure 4. Percentage of graphene etched area at different temperatures: (a) 700 °C; (b) 800 °C; (c) 900 °C; (d) 1000 °C. Five regions were randomly picked for the calculation of etched area; each region is 40 μm × 30 μm. (e) Etched area *versus* temperature plot.

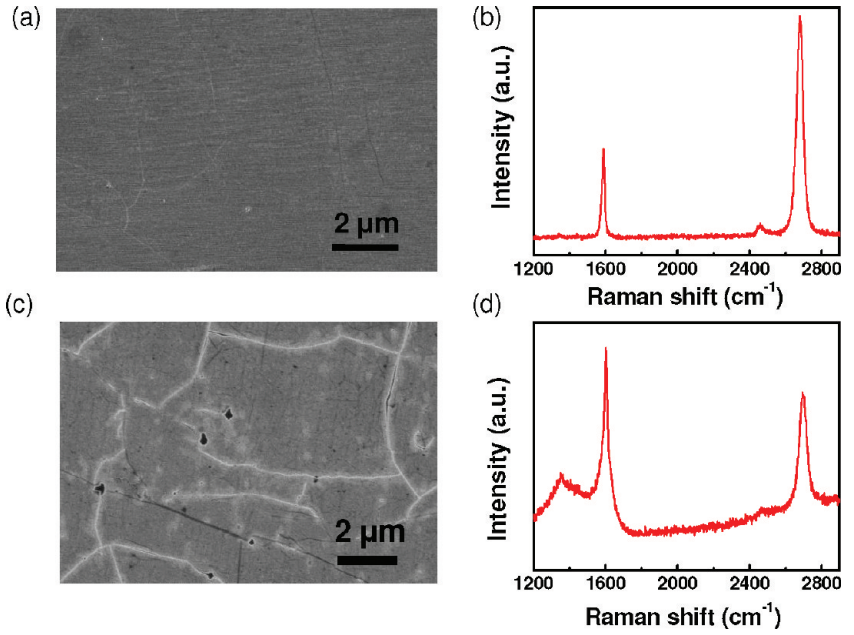

Figure 5. (a) SEM image of CVD graphene transferred onto a Si/SiO_2 substrate. (b) Representative Raman spectrum of SLG. (c) SEM image of transferred CVD graphene after H_2 annealing at 800 °C. (d) Representative Raman spectrum of CVD graphene after H_2 annealing.

from 800 °C to 1000 °C. In Figure 4e, we calculated the mean values of the etched area of graphene at different temperatures, and it could be clearly seen that the percentage of etched area increased from 25% at 700 °C to 58% at 800 °C, then dropped to 49% at 900 °C, and further decreased to 30% at 1000 °C.

In order to confirm the catalytic function of a copper substrate, a further experiment was carried out for comparison. We loaded our transferred graphene sample into the same CVD system, and the sample was kept at 800 °C for 30 min with a flow of 30 sccm H_2. The system pressure was maintained at 500 mTorr during the process. Figure 5a is the SEM image of as-grown CVD graphene after transfer, which is continuous and uniform over a large area. A typical Raman spectrum of the transferred graphene is shown in Figure 5b, which is almost identical to the Raman spectrum in the inset of Figure 2a, indicating SLG with very low defect density. After annealing in hydrogen, we did not observe any obvious anisotropic etched patterns on graphene. The white lines in Figure 5c should be due to the formation of wrinkles in graphene due to the thermal cycling.

The Raman spectrum in Figure 5d was taken from the sample after hydrogen annealing, which showed a strong D peak at ~1350 cm^{-1}, which can be attributed to disorder in graphene.[30] Also, the Raman spectra showed broadening of the G and 2D peaks, as well as a decrease of intensity of the 2D peak, indicating the graphene has become more defective after annealing in hydrogen. Altogether, we can conclude that the etching reaction is catalyzed by copper and the anisotropic etching would not happen if there is no copper participating in the reaction.

The anisotropic property of the catalytic etching can be applied to determine the crystalline orientation of CVD graphene and to estimate the grain size of graphene. If the hexagonal etched patterns are parallel to each other within a certain area, one can conclude that the area should be within a single graphene grain. We can use the SEM image in Figure 1c as an example. The hexagonal patterns are well aligned with each other over the inspected area, and hence an area of more than ~6 μm × 2 μm should be one single graphene grain. In comparison, in Figure 2b the bottom left etched pattern is not parallel to the middle three hexagonal etched patterns, which implies that the bottom left part of the graphene may have a different crystalline orientation from the graphene grain containing the middle three etched hexagons. This simple etching method provides a useful tool to estimate the grain size of graphene, as compared to more sophisticated technologies such as scanning tunneling microscopy (STM),[14] transmission electron microscopy (TEM),[31,32] and low-energy electron microscopy (LEEM).[15,33]

Studying the etching reaction also helps to better understand and control the graphene growth conditions. We can also observe the hexagonal etched patterns on the as-grown graphene if we turn methane off after 30 min of graphene growth, with only hydrogen flowing in the CVD system during the cooling process. This phenomenon indicates that the graphene growth and hydrogen etching are competitive with each other. The graphene growth reaction is endothermic and will happen and reach equilibrium only when the temperature increases to a certain point. During the cooling

process, the former equilibrium breaks and the reaction shifts from graphene growth to hydrogen etching at a certain temperature, since the etching reaction is exothermic and will be more favorable when the temperature decreases. Our observation suggests that one should keep methane flowing during the cooling process to suppress hydrogen etching in order to grow continuous CVD graphene films.

In summary, we have developed an anisotropic hydrogen etching method of graphene catalyzed by the copper substrate. The anisotropic etching is the reverse reaction of CVD graphene growth, and it is simple, clean, and highly efficient at 800 °C and 500 mTorr with hydrogen gas flow. Of the 139 angles measured at graphene edges after etching, 80% are 120°, and the etched edges are confirmed to be along the ⟨1120⟩ zigzag direction. Moreover, we observed that copper played an important role in catalyzing the etching reaction, as no etching was observed for graphene transferred to Si/SiO_2 under similar conditions. This highly anisotropic hydrogen etching technology may work as a simple and convenient way to determine graphene grain size and crystal orientation and may enable the etching of graphene into nanoribbons for electronic applications.

METHODS

Graphene growth was done using copper foil (99.8%, Alpha Aesar) as a substrate. Copper foil was loaded into a 2 in. fused quartz tube and heated to 1000 °C with the flow of 7 sccm H_2 at 40 mTorr. The Cu foil was then annealed at 1000 °C for 20 min. Seven sccm CH_4 and 30 sccm H_2 were introduced to the CVD system at 500 mTorr for 30 min for graphene growth. The temperature was decreased to 600 °C without changing flow rates and pressure. CH_4 was then turned off at 600 °C, and the system was cooled to room temperature with the flow of 30 sccm H_2 at 500 mTorr. Anisotropic etching of graphene by hydrogen was done in the same CVD chamber as graphene growth, with the flow of 30 sccm H_2 at 500 mTorr, and the etching was carried out for 30 min at 800 °C.

Micro-Raman characterization was done by using an inVia Renishaw Raman instrument. Raman spectra were obtained with 532 nm laser excitation.

Acknowledgment. We acknowledge financial support from the Focus Center Research Program (FCRP), Center on Functional Engineered Nano Architectonics (FENA), the King Abdul Aziz City for Science and Technology (KACST)/California Center of Excellence on Nano Science and Engineering for Green and Clean Technologies. We thank Professor Stephen Cronin for access to micro-Raman system.

Supporting Information Available: Figure S1: EDX spectra on different areas of graphene sample after etching. Figure S2: Raman spectra and D band intensity in graphene and at etched edges. This material is available free of charge via the Internet http://pubs.acs.org.

REFERENCES AND NOTES

1. Geim, A. K.; Novoselov, K. S. The Rise of Graphene. *Nat. Mater.* **2007**, *6*, 183–191.
2. Novoselov, K. S.; Geim, A. K.; Morozov, S. V.; Jiang, D.; Zhang, Y.; Dubonos, S. V.; Grigorieva, I. V.; Firsov, A. A. Electric Field Effect in Atomically Thin Carbon Films. *Science* **2004**, *306*, 666–669.
3. Bolotin, K. I.; Ghahari, F.; Shulman, M. D.; Stormer, H. L.; Kim, P. Observation of the Fractional Quantum Hall Effect in Graphene. *Nature* **2009**, *462*, 196–199.
4. Karu, A. E.; Beer, M. Pyrolytic Formation of Highly Crystalline Graphite Films. *J. Appl. Phys.* **1966**, *37*, 2179.
5. Yu, Q. K.; Lian, J.; Siriponglert, S.; Li, H.; Chen, Y. P.; Pei, S. S. Graphene Segregated on Ni Surfaces and Transferred to Insulators. *Appl. Phys. Lett.* **2008**, *93*, 113103.
6. Reina, A.; Jia, X. T.; Ho, J.; Nezich, D.; Son, H. B.; Bulovic, V.; Dresselhaus, M. S.; Kong, J. Large Area, Few-Layer Graphene Films on Arbitrary Substrates by Chemical Vapor Deposition. *Nano Lett.* **2009**, *9*, 30–35.
7. Kim, K. S.; Zhao, Y.; Jang, H.; Lee, S. Y.; Kim, J. M.; Kim, K. S.; Ahn, J. H.; Kim, P.; Choi, J. Y.; Hong, B. H. Large-Scale Pattern Growth of Graphene Films for Stretchable Transparent Electrodes. *Nature* **2009**, *457*, 706–710.
8. De Arco, L. G.; Zhang, Y.; Kumar, A.; Zhou, C. W. Synthesis, Transfer, and Devices of Single- and Few-Layer Graphene by Chemical Vapor Deposition. *IEEE T. Nanotechnol.* **2009**, *8*, 135–138.
9. Li, X. S.; Cai, W. W.; An, J. H.; Kim, S.; Nah, J.; Yang, D. X.; Piner, R.; Velamakanni, A.; Jung, I.; Tutuc, E. Large-Area Synthesis of High-Quality and Uniform Graphene Films on Copper Foils. *Science* **2009**, *324*, 1312–1314.
10. Levendorf, M. P.; Ruiz-Vargas, C. S.; Garg, S.; Park, J. Transfer-Free Batch Fabrication of Single Layer Graphene Transistors. *Nano Lett.* **2009**, *9*, 4479–4483.
11. Zhang, Y.; Gomez, L.; Ishikawa, F. N.; Madaria, A.; Ryu, K.; Wang, C. A.; Badmaev, A.; Zhou, C. W. Comparison of Graphene Growth on Single-Crystalline and Polycrystalline Ni by Chemical Vapor Deposition. *J. Phys. Chem. Lett.* **2010**, *1*, 3101–3107.
12. Bhaviripudi, S.; Jia, X. T.; Dresselhaus, M. S.; Kong, J. Role of Kinetic Factors in Chemical Vapor Deposition Synthesis of Uniform Large Area Graphene Using Copper Catalyst. *Nano Lett.* **2010**, *10*, 4128–4133.
13. Li, X. S.; Cai, W. W.; Colombo, L.; Ruoff, R. S. Evolution of Graphene Growth on Ni and Cu by Carbon Isotope Labeling. *Nano Lett.* **2009**, *9*, 4268–4272.
14. Yu, Q. K.; Jauregui, L. A.; Wu, W.; Colby, R.; Tian, J. F.; Su, Z. H.; Cao, H. L.; Liu, Z. H.; Pandey, D.; Wei, D. G. Control and Characterization of Individual Grains and Grain Boundaries in Graphene Grown by Chemical Vapour Deposition. *Nat. Mater.* **2011**, *10*, 443–449.
15. Li, X. S.; Magnuson, C. W.; Venugopal, A.; Tromp, R. M.; Hannon, J. B.; Vogel, E. M.; Colombo, L.; Ruoff, R. S. Large-Area Graphene Single Crystals Grown by Low-Pressure Chemical Vapor Deposition of Methane on Copper. *J. Am. Chem. Soc.* **2011**, *133*, 2816–2819.
16. Vlassiouk, I.; Regmi, M.; Fulvio, P.; Dai, S.; Datskos, P.; Eres, G.; Smirnov, S. Role of Hydrogen in Chemical Vapor Deposition Growth of Large Single-Crystal Graphene. *ACS Nano* **2011**, *5*, 6069–6076.
17. Wang, X. R.; Dai, H. J. Etching and Narrowing of Graphene From the Edges. *Nat. Chem.* **2010**, *2*, 661–665.
18. Yang, R.; Zhang, L. C.; Wang, Y.; Shi, Z. W.; Shi, D. X.; Gao, H. J.; Wang, E. G.; Zhang, G. Y. An Anisotropic Etching Effect in the Graphene Basal Plane. *Adv. Mater.* **2010**, *22*, 4014–4019.
19. Zhang, G. Y.; Shi, Z. W.; Yang, R.; Zhang, L. C.; Wang, Y.; Liu, D. H.; Shi, D. X.; Wang, E. G. Patterning Graphene with Zigzag Edges by Self-Aligned Anisotropic Etching. *Adv. Mater.* **2011**, *23*, 3061.
20. Ryu, K.; Badmaev, A.; Gomez, L.; Ishikawa, F.; Lei, B.; Zhou, C. W. Synthesis of Aligned Single-Walled Nanotubes Using

Catalysts Defined by Nanosphere Lithography. *J. Am. Chem. Soc.* **2007**, *129*, 10104.
21. Gupta, A. K.; Russin, T. J.; Gutierrez, H. R.; Eklund, P. C. Probing Graphene Edges via Raman Scattering. *ACS Nano* **2009**, *3*, 45–52.
22. Jiao, L. Y.; Wang, X. R.; Diankov, G.; Wang, H. L.; Dai, H. J. Facile Synthesis of High-Quality Graphene Nanoribbons. *Nat. Nanotechnol.* **2010**, *5*, 321–325.
23. Baker, R. T. K.; Chludzinski, J. J. Catalytic Gasification of Graphite by Chromium and Copper in Oxygen, Steam and Hydrogen. *Carbon* **1981**, *19*, 75–82.
24. Campos, L. C.; Manfrinato, V. R.; Sanchez-Yamagishi, J. D.; Kong, J.; Jarillo-Herrero, P. Anisotropic Etching and Nanoribbon Formation in Single-Layer Graphene. *Nano Lett.* **2009**, *9*, 2600–2604.
25. Ci, L.; Xu, Z. P.; Wang, L. L.; Gao, W.; Ding, F.; Kelly, K. F.; Yakobson, B. I.; Ajayan, P. M. Controlled Nanocutting of Graphene. *Nano Res.* **2008**, *1*, 116–122.
26. Goethel, P. J.; Yang, R. T. Mechanism of Graphite Hydrogenation Catalyzed by Nickel. *J. Catal.* **1987**, *108*, 356–363.
27. Goethel, P. J.; Yang, R. T. The Tunneling Action of Group-VIII Metal Particles in Catalyzed Graphite Hydrogenation. *J. Catal.* **1988**, *114*, 46–52.
28. Ren, W. C.; Gao, L. B.; Liu, B. L.; Wu, Z. S.; Jiang, C. B.; Cheng, H. M. Crystallographic Tailoring of Graphene by Nonmetal SiO(x) Nanoparticles. *J. Am. Chem. Soc.* **2009**, *131*, 13934.
29. Pan, Z. J.; Yang, R. T. The Mechanism of Methane Formation from the Reaction between Graphite and Hydrogen. *J. Catal.* **1990**, *123*, 206–214.
30. Dresselhaus, M. S.; Jorio, A.; Hofmann, M.; Dresselhaus, G.; Saito, R. Perspectives on Carbon Nanotubes and Graphene Raman Spectroscopy. *Nano Lett.* **2010**, *10*, 751–758.
31. Huang, P. Y.; Ruiz-Vargas, C. S.; Van der Zande, A. M.; Whitney, W. S.; Levendorf, M. P.; Kevek, J. W.; Garg, S.; Alden, J. S.; Hustedt, C. J.; Zhu, Y. Grains and Grain Boundaries in Single-Layer Graphene Atomic Patchwork Quilts. *Nature* **2011**, *469*, 389.
32. Kim, K.; Lee, Z.; Regan, W.; Kisielowski, C.; Crommie, M. F.; Zettl, A. Grain Boundary Mapping in Polycrystalline Graphene. *ACS Nano* **2011**, *5*, 2142–2146.
33. Wofford, J. M.; Nie, S.; McCarty, K. F.; Bartelt, N. C.; Dubon, O. D. Graphene Islands on Cu Foils: The Interplay between Shape, Orientation, and Defects. *Nano Lett.* **2010**, *10*, 4890–4896.